PAPER

Adaptive Channel Estimation for Coherent DS-CDMA Mobile Radio Using Time-Multiplexed Pilot and Parallel Pilot Structures

Sadayuki ABETA†, Mamoru SAWAHASHI†, *and* Fumiyuki ADACHI†, *Members*

SUMMARY Adaptive channel estimation filters are presented for coherent DS-CDMA reverse link using time-multiplexed pilot and parallel pilot structures. Fast transmit power control (TPC) is adopted in the reverse link. Fading statistical properties are not preserved when fast TPC is used. When fading is slow, the channel is similar to non-fading channel, but its starts to vary as fading become faster since fast TPC cannot track fading perfectly. A pragmatic approach is used in this paper to derive adaptive channel estimation filter. The filter coefficients are updated based on the measured autocorrelation function of the instantaneous channel estimate. The bit error rate (BER) performance under frequency selective Rayleigh fading is evaluated by computer simulation to show that the adaptive channel estimation filter provides superior performance to the previously proposed non-adaptive WMSA filter.

key words: *adaptive channel estimation, DS-CDMA, pilot channel, coherent RAKE*

1. Introduction

Wideband wireless access based on direct sequence code division multiple access (W-CDMA) is considered to be the most promising access scheme for 3rd generation mobile radio systems called IMT-2000 [1]-[8]. The link capacity is inverse proportionate to the required signal energy-to-noise (plus interference) power spectrum density ratio (E_b/N_0) and therefore, coherent detection that requires less E_b/N_0 than noncoherent detection is desirable in W-CDMA. For coherent detection, accurate channel estimation is necessary under fast multipath fading environment. Since, in the reverse (mobile-to-cell cite) link, the multiple access interference (MAI) is caused by the large differences in received signal powers transmitted from different users resulting from the well known near/far problem and fast fading, the reverse link requires fast transmit power control (TPC) so that all signals transmitted from different users are received with almost equal power at a cell site receiver. Since the fading channel statistical properties are not preserved by fast TPC, the channel estimation filter based on Wiener filter theory cannot be applied to the reverse links.

The pilot channel-assisted channel estimation scheme offers good tracking performance against fast fading [9]-[13]. Basically, there are two types of pilot channel structure. One is the time-multiplexed pilot where known pilot symbols are periodically multiplexed into the transmitted data symbol sequence. A pragmatic solution called weighted multi-slot averaging (WMSA) channel estimation filter was proposed in [14] for the case of time-multiplexed pilot channel structure. In WMSA channel estimation, instantaneous channel estimate is obtained by simple averaging of pilot symbols belonging to each slot (each slot consist of pilot symbols followed by date symbols) and then, smoothed by a smoothing filter over 2K slots. The WMSA channel estimation filter yields better BER performance than a linear interpolation filter and a simple two-slot averaging filter [10] that averages the pilot symbols belonging to two consecutive slots. The constant weights or filter coefficients are determined by a cut and try approach so that a good performance is achieved over a wide range of fading maximum Doppler frequency f_D (or terminal traveling speed). However, since optimum filter coefficients exist at each value of f_D, it is desirable to adopt filter coefficients to changing value of f_D. The other type is the parallel pilot channel structure where known pilot symbol sequences are parallel-multiplexed using orthogonal spreading sequence structure [12]. The idea of WMSA channel estimation filter can be also applied to the parallel pilot channel.

This paper proposes adaptive channel estimation filters for time-multiplexed and parallel pilot structures. After describing the coherent RAKE receiver structure with the channel estimation filter in Sect. 2, Sect. 3 describes adaptive WMSA channel estimation filter for time-multiplex pilot channel structure. Section 4 describes adaptive channel estimation filter for parallel pilot channel structure. Section 5 optimizes, by the means of computer simulation, the observation time interval pilot for channel estimation filter and compares the achievable BER performance with that of previously proposed WMSA of both pilot channel structures.

2. Coherent RAKE Receiver Structure

2.1 Received Signal

We assume that the binary information data sequence of one frame is first convolutional coded, bit-interleaved and then, QPSK-modulated. In the case of the time-multiplexed pilot channel, the QPSK symbol sequence is mapped over a sequence of slots, each containing N_d data symbols preceded by N_p pilot symbols placed at the beginning of each slot (see

Manuscript received November 14, 1998.
Manuscript revised April 17, 1999.

† The authors are with Wireless Laboratories, NTT Mobile Communications Network Inc., YRP, Yokosuka-shi, 239-8536 Japan.

Fig. 1). The resultant symbol sequence is spread over much wider bandwidth by a spreading sequence. The slot length $T_{slot} = (N_p + N_d)T$, where T is the QPSK symbol duration. In the case of the parallel pilot channel, on the other hand, data and pilot channels are spread by orthogonal spreading sequences.

Assuming that the multiple channel has $L(\geq 1)$ resolvable, frequency-nonselective path, the spread signal received over a multipath channel can be represented as

$$r(t) = \sum_{l=0}^{L-1} r_l(t) = \sqrt{2S} \sum_{l=0}^{L-1} \xi_l(t) s(t-\tau_l) + \rho(t), \tag{1}$$

where S is the average received signal power, $r(t)$ is the background noise (plus MAI), $\xi_l(t)$ and τ_l are the complex-valued channel gain and time delay of the l-th path (l=0,1,..., L–1), respectively, and $s(t)$ is the transmitted spread signal waveform. We assume $\mathrm{E}\left[\sum_{l=1}^{L-1} |\xi_l(t)|^2\right] = 1$, where E[.] denotes ensemble average and E[$|s(t)|^2$]=1. $s(t)$ can be represented as

$$s(t) = \begin{cases} g_{tm}(t) d_{tm}(t) \\ \quad \text{for time - miltiplexed pilot channel structure} \\ \\ g_{pd}(t) d_p(t) + g_{pp}(t) p_p(t) \\ \quad \text{for parallel pilot channel structure} \end{cases} \tag{2}$$

In Eq. (2), $g_{tm}(t)$ and $d_{tm}(t)$ are the spreading waveform and QPSK modulated signal waveform including the pilot data in the case of the time-multiplexed pilot channel case, respectively. $g_{pd}(t)$ and $g_{pp}(t)$ are the orthogonal spreading waveforms for data channel and pilot channel in the case of the parallel pilot channel case, respectively, $d_p(t)$ is the QPSK modulated data waveform, and $p_p(t)$ is the pilot signal waveform. They can be represented as

$$\begin{cases} g_{tm}(t) = \sum_{i=-\infty}^{\infty} c_{tm}(i) u(t/T_c - i) \\ d_{tm}(t) = \sum_{k=-\infty}^{\infty} \exp[j\phi_{tm}(k)] u(t/T - k) \end{cases} \tag{3}$$

$$\begin{cases} g_{pd}(t) = \sum_{i=-\infty}^{\infty} c_{pd}(i) u(t/T_c - i), \\ g_{pp}(t) = \sum_{i=-\infty}^{\infty} c_{pp}(i) u(t/T_c - i) \\ d_p(t) = \sum_{k=-\infty}^{\infty} \exp[j\phi_p(k)] u(t/T - k), \\ p_p(t) = \sum_{k=-\infty}^{\infty} \sqrt{\zeta}\, u(t/T - k) \end{cases} \tag{4}$$

where $c_{tm}(i)$ is the spreading sequence, $c_{pd}(i)$ and $c_{pp}(i)$ are the orthogonal binary spreading sequences, $\phi_{tm}(k)$ and $\phi_p(k) \in \{(2m+1)\pi/4;\, m = 0-3\}$ are the QPSK modulation phases, ζ is the power factor of the pilot channel relative to the data channel, T_c is the chip duration of the spreading sequence, T/T_c represents the processing gain, and $u(t)$ is the unit function.

2.2 Coherent RAKE Combining and Channel Decoding

Figures 2 show block diagrams of the coherent RAKE receiver with channel estimation filter for the time-multiplexed pilot channel structure (a) and parallel pilot channel structure (b). The received signal is despread by a matched filter and resolved into the L QPSK signals that have propagated along different frequency-nonselective paths with different time delays. The matched filter output at the m-th symbol position of n-th slot associated with the l-th path can be represented as

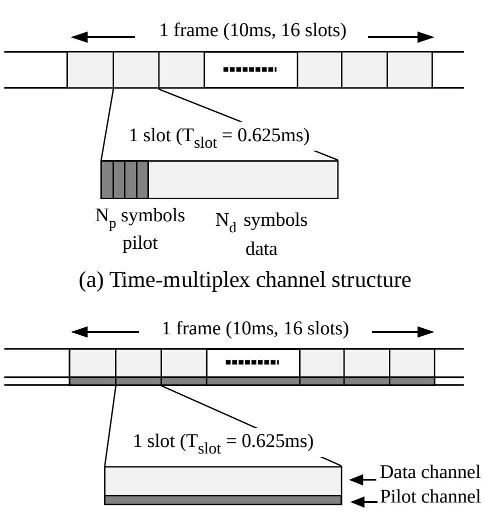

(a) Time-multiplex channel structure

(b) Parallel pilot channel structure

Fig. 1 Channel structures.

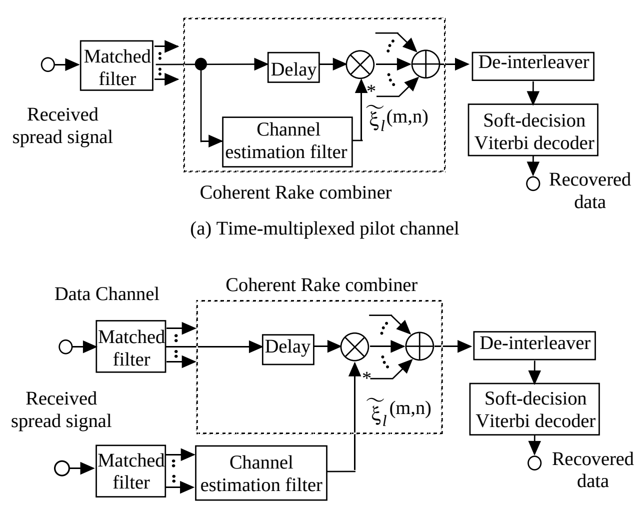

(a) Time-multiplexed pilot channel

(b) parallel pilot channel

Fig. 2 Block diagrams of coherent RAKE receivers.

$$r_l(m,n)=\frac{1}{T}\int_{mT+nT_{slots}+\tau_l}^{(m+1)T+nT_{slots}+\tau_l} r_l(t)g(t-\tau_l)dt \tag{5}$$

$$=\sqrt{2S}\,\xi_l(m,n)\exp j\phi_{tm}(m,n)+\rho_l(m,n)$$

for time-multiplexed pilot channel structure (6a)

$$=\begin{cases}\sqrt{2S}\,\xi_l(m,n)\exp j\phi_p(m,n)+\rho_l(m,n)\,, & \text{data channel}\\ \sqrt{2S}\,\xi_l(m,n)\zeta+\rho_l(m,n)\,, & \text{pilot channel}\end{cases}$$

for parallel pilot channel structure (6b)

where $g(t)=\{g_{tm}(t),g_{pd}(t),g_{pp}(t)\}$, $\xi_l(m,n)=\xi_l(mT+nT_{slot})$, $\phi_{tm}(m,n)=\phi_{tm}(mT+n(N_D+N_p))$, $\phi_p(m,n)=\phi_p(mT+nN_D)$, and $\rho_l(m,n)$ is the noise component (note that the noise component is different for three cases in Eq. (6)). The channel estimation filter, which is described in Sect. 3, is to estimate the value of $\xi_l(m,n)$ using the pilot channel and its estimate is denoted by $\tilde{\xi}_l(m,n)$. L despread and resolved signal components are multiplied by the complex conjugates of $\tilde{\xi}_l(m,n)$'s before being combined (maximal-ratio combing (MRC)). The RAKE combiner output at the m-th symbol position of n-th slot is therefore, represented as

$$\bar{d}(m,n)=\sum_{l=0}^{L-1} r_l(m,n)\tilde{\xi}_l^*(m,n)\,, \tag{7}$$

where * denotes the complex conjugate. Finally, the RAKE combiner output is de-interleaved and soft-decision Viterbi decoded to recover the transmitted data.

3. Adaptive WMSA Channel Estimation Filter for Time-Multiplexed Pilot Channel Structure

Since the values of $\xi_l(t)$'s remains almost constant over a period of N_p pilot symbols, the simple accumulation of N_p consecutive pilot symbols improves the signal-to-noise (including MAI) power ratio (SNR). The estimate of instantaneous channel gain at the beginning of the n-th slot of the l-th path is given by

$$\hat{\xi}_l(t)=\frac{1}{N_p}\sum_{m=0}^{N_p-1} r_l(m,n)\exp(-j\pi/4)\,. \tag{8}$$

In the case of very slow fading, we can extend the observation interval to several slots and coherently add several consecutive instantaneous channel estimates to further increase SNR. However, in general, the propagation channel gain varies slot-by-slot. Therefore, the instantaneous channel estimates $\tilde{\xi}_l(n)$ need to be smoothed by a smoothing filter (see Fig. 3). Hereafter, we introduce a new parameter $m'=m+N_p$ to represent the data symbol position (note that m represents data position for parallel pilot channel structure) The smoothing filter output is expressed as

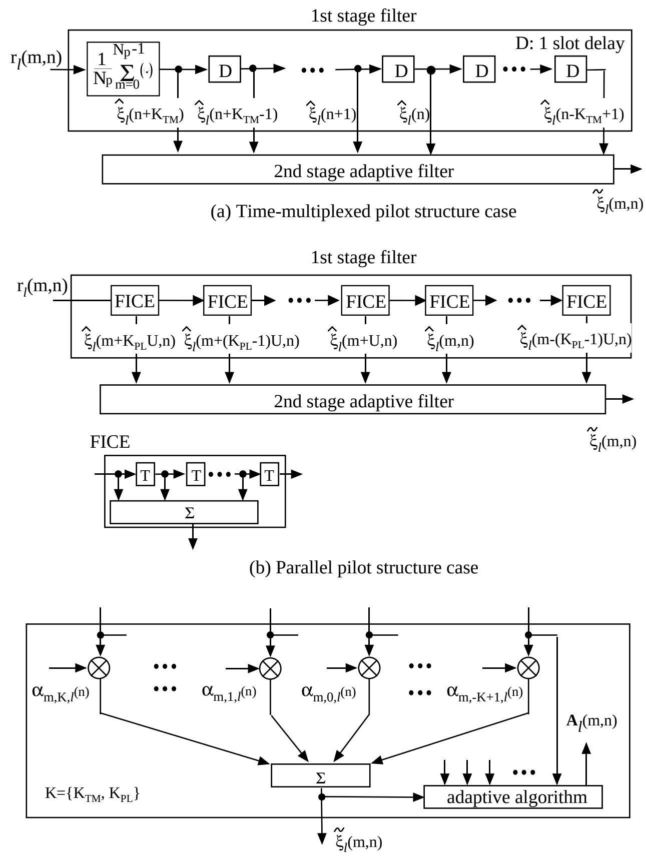

(a) Time-multiplexed pilot structure case

(b) Parallel pilot structure case

(c) 2nd stage adaptive filter

Fig. 3 Adaptive channel estimator.

$$\tilde{\xi}_l(m',n)=\sum_{v=-K_{TM}+1}^{K_{TM}}\alpha_{m',v,l}(n)\hat{\xi}_l(n+v)\,, \tag{9}$$

where $\alpha_{m',v,l}(n)$ is the real-valued filter coefficient of the $(n+v)$-th instantaneous channel estimate for obtaining the channel estimate at m'-th data position of n-th slot for l-th path and $2K_{TM}$ is the observation interval represented by the number of slots. For the original smoothing filter called WMSA channel estimation filter [14], we used $\alpha_{m',v,l}(n)=\alpha_v(n)$ for all m' and l and $\{\alpha_v(n)\}$ were determined using a cut and try approach by a computer simulation. Figures 3 show the block diagrams of our proposed adaptive WMSA channel estimation filter. The bandwidth of smoothing filter needs to be as much as narrow but sufficiently wide enough not to distort the fading power spectrum. Since the fading maximum Doppler frequency f_D changes according to the change in the terminal travelling speed, the filter coefficient $\alpha_{m',v,l}(n)$ must be adaptively determined. As f_D increases, the bandwidth of smoothing filter must become wider (i.e. the filter coefficient $\alpha_{m',v,l}(n)$'s must fall down more quickly as |n| increase). Again, we follow a pragmatic approach by exploiting the fact that as fading becomes faster, the autocorrelation function of the fading process perturbed by fast TPC falls off faster.

We define the filter coefficient $\alpha_{m',v,l}(n)$ at 3 positions

m'=0, $N_d/2$ and N_d-1, which are to be estimates by the adaptive algorithm in this paper, and then linear-interpolate them to obtain $\alpha_{m',v,l}(n)$ for all m' in Eq. (9):

$$\alpha_{m',v,l}(n) = \begin{cases} \dfrac{(N_d/2-m')\alpha_{0,v,l}(n)+m'\alpha_{N_d/2,v,l}(n)}{N_d/2}, & \text{for } 0 \le m' \le N_d/2 \\ \dfrac{(N_d-1-m')\alpha_{N_d/2,v,l}(n)+(m'-N_d/2)\alpha_{N_d-1,v,l}(n)}{N_d/2-1}, & \text{for } N_d/2 < m' \le N_d-1 \end{cases} \tag{10}$$

First, how to update $\alpha_{N_d/2,v,l}(n)$ $(=\alpha_{m'=N_d/2,v,l}(n))$ of Eq. (10) is described below. Let $\hat{\mathbf{X}}_l(n)$ be the vector of the estimated instantaneous channel gains obtained by the 1st stage filter which is defined as

$$\hat{\mathbf{X}}_l(n) = \begin{pmatrix} \hat{\xi}_l(n-K_{TM}+1) \\ \hat{\xi}_l(n-K_{TM}+2) \\ \vdots \\ \hat{\xi}_l(n) \\ \vdots \\ \hat{\xi}_l(n+K_{TM}-1) \\ \hat{\xi}_l(n+K_{TM}) \end{pmatrix}. \tag{11}$$

Furthermore, we denote $\mathbf{A}_l(N_d/2, n)$ as the vector of the filter coefficients $\{\alpha_{N_d/2,v,l}(n)\}$, they are defined as

$$\mathbf{A}_l(N_d/2,n) = \begin{pmatrix} \alpha_{N_d/2,-K_{TM}+1,l}(n) \\ \alpha_{N_d/2,-K_{TM}+2,l}(n) \\ \vdots \\ \alpha_{N_d/2,0,l}(n) \\ \vdots \\ \alpha_{N_d/2,K_{TM}-1,l}(n) \\ \alpha_{N_d/2,K_{TM},l}(n) \end{pmatrix}, \tag{12}$$

$$\overline{\mathbf{A}}_l(N_d/2,n) = \begin{pmatrix} \overline{\alpha}_{N_d/2,-K_{TM}+1,l}(n) \\ \overline{\alpha}_{N_d/2,-K_{TM}+2,l}(n) \\ \vdots \\ \overline{\alpha}_{N_d/2,0,l}(n) \\ \vdots \\ \overline{\alpha}_{N_d/2,K_{TM}-1,l}(n) \\ \overline{\alpha}_{N_d/2,K_{TM},l}(n) \end{pmatrix}, \tag{13}$$

where

$$\overline{\alpha}_{N_d/2,v,l}(n) = \overline{\alpha}_{N_d/2,1-v,l}(n) = \frac{\alpha_{N_d/2,v,l}(n)+\alpha_{N_d/2,1-v,l}(n)}{2}. \tag{14}$$

$\mathbf{A}_l(N_d/2, n)$ is updated and as

$$\overline{\mathbf{A}}_l\left(\frac{N_d}{2},n-1\right)+\mu\eta_l(n) \to \overline{\mathbf{A}}_l\left(\frac{N_d}{2},n\right)$$
$$\frac{\overline{\mathbf{A}}_l\left(\frac{N_d}{2},n\right)}{\sum_{v=-K_{TM}+1}^{K_{TM}} \alpha_{N_d/2,v,l}(n)} \to \overline{\mathbf{A}}_l\left(\frac{N_d}{2},n\right), \tag{15}$$

where m $(0<m<1)$ is the update factor and

$$\eta_l(n) = \hat{\mathbf{X}}_l(n)\cdot\overline{\xi}^*(N_d/2,n) \tag{16}$$

is the $2K_{TM}$-element vector representing the cross-correlation function of the instantaneous channel estimate with respect to the filter output $\overline{\xi}_l(N_d/2,n)$ which is obtained by using $\overline{\mathbf{A}}_l(N_d/2,n-1)$ instead of $\mathbf{A}_l(N_d/2,n)$, i.e.,

$$\overline{\xi}_l(N_d/2,n) = \overline{\mathbf{A}}_l^T(N_d/2,n-1)\hat{\mathbf{X}}_l(n), \tag{17}$$

where $(.)^T$ is a transpose. When the value of f_D increases, some of the elements of $\eta_l(n)$ may have negative values and consequently $\overline{\alpha}_{N_d/2,v,l}(n)$ may become negative. When this happens, $\overline{\alpha}_{N_d/2,v,l}(n)$ is replaced with zero in Eq. (14). Since, the fading auto correlation function is an even function, the filter coefficients, $\alpha_{N_d/2,1-v,l}(n)$ and $\alpha_{N_d/2,v,l}(n)$, should be equal in average sense and therefore, this constraint is applied to secure the convergence of the filter coefficient vector, the sum of the filter coefficients of $\mathbf{A}_l(N_d/2,n)$ is normalized to unity in Eq. (15). It is obvious that the value of n-th element, $-K_{TM}+1 \le n \le K_{TM}$ of $\eta_l(n)$ fall off more quickly as $|n|$ increase for faster fading (or larger f_D value). As previously mentioned, the filter coefficients must have the same property. Therefore this fact is exploited in obtaining algorithm of Eq. (15).

$\alpha_{0,v,l}(n)$ and $\alpha_{N_d-1,v,l}(n)$ are updated by the same algorithm as for $\alpha_{N_d/2,v,l}(n)$ by just replacing the symbol position $m'=N_d/2$ with m'=0 and N_d-1, respectively in Eqs. (12)–(17). In the case of $m'=N_d/2$, a pair of instantaneous channel estimates, $\hat{\xi}_l(n-v+1)$ and $\hat{\xi}_l(n+v)$ should equally contribute to the filter output because their time distances from the time position of $m'=N_d/2$ are the almost same. Therefore, $2K_{TM}$ instantaneous channel estimates, $n=-K_{TM}+1,\cdots, 0,1,\cdots, K_{TM}$ are involved in Eqs. (14) and (15). However, in the case of m'=0 (N_d-1), equally distances in time from the time position of m'=0 (N_d-1) are a pair of instantaneous channel estimates, $\hat{\xi}_l(n-v)$ and $\hat{\xi}_l(n+v)$ ($\hat{\xi}_l(n-v+2)$ and $\hat{\xi}_l(n+v)$). Therefore, $2K_{TM}-1$ instantaneous channel estimates, $n=-K_{TM}+1,\cdots, 0,1,\cdots, K_{TM}-1$ $(=-K_{TM}+2,\cdots, 0,1,\cdots,K_{TM})$, are involved in Eqs. (14) and (15). This is done by letting $\alpha_{0,K_{TM},l}(n)=0$ for m'=0 case and $\alpha_{0,-K_{TM}+1,l}(n)=0$ for $m'=N_d-1$ case.

4. Adaptive Channel Estimation Filter for Parallel Pilot Channel Structure

In the parallel pilot channel structure shown in Fig. 3(b), we can also extend the observation interval to increase the SNR. The outputs of matched filter are first coherently summed over U pilot symbols to estimate the instantaneous channel gain at the FICE (first instantaneous channel estimator) stage. The n-th channel estimate is given by

$$\hat{\xi}_l(m+vU,n)=\frac{1}{U}\sum_{i=0}^{U-1} r_l(m+i+(v-1)U,n)\exp(-j\pi/4), \tag{18}$$

To smooth the instantaneous channel estimate, $\hat{\xi}_l(m+vU,n)$'s are weighted and summed by a smoothing filter as in the case of time-multiplexed pilot channel. The filter output is represented as

$$\tilde{\xi}_l(m,n)=\frac{1}{2K_{PL}}\sum_{v=-K_{PL}+1}^{K_{PL}}\alpha_{m,v,l}(n)\hat{\xi}_l(m+vU,n)\ , \tag{19}$$

where $\alpha_{m,v,l}(n)$ is the real-valued filter coefficient and $2K_{PL}$ is the observation interval (the time interval is given by $2K_{PL} \times U$ symbols). In Fig. 3(a), the shift registers of adaptive WMSA channel estimation filter are updated slot-by-slot, i.e., the same measured instantaneous channel estimates $\hat{\xi}_l(n)$'s are used for obtaining $\hat{\xi}_l(m,n)$at all symbol positions within n-th the slot. In Fig. 3(b), on the other hand, the shift registers are updated symbol-by-symbol. The optimum filter coefficients $\alpha_{m,v,l}(n)$ are updated based on the same idea used in time-multiplexed pilot channel structure.

Let $\hat{\mathbf{X}}_l(m,n)$ be the vector of the estimated instantaneous channel gains obtained by the 1st stage filter which is defined as

$$\hat{\mathbf{X}}_l(n)=\begin{pmatrix}\hat{\xi}_l(m-(K_{PL}-1)U,n)\\ \hat{\xi}_l(m-(K_{PL}-2)U,n)\\ \vdots\\ \hat{\xi}_l(m,n)\\ \vdots\\ \hat{\xi}_l(m+(K_{PL}-1)U,n)\\ \hat{\xi}_l(m+K_{PL}U,n)\end{pmatrix}. \tag{20}$$

Furthermore, we denote $\mathbf{A}_l(m, n)$ as vector of the filter coefficients $\{a_{m,n,l}(n)\}$ and $\overline{\mathbf{A}}_l(m,n)$ as the averaged filter coefficient vector. They are defined as

$$\mathbf{A}_l(m,n)=\begin{pmatrix}\alpha_{m,-K_{PL}+1,l}(n)\\ \alpha_{m,-K_{PL}+2,l}(n)\\ \vdots\\ \alpha_{m,0,l}(n)\\ \vdots\\ \alpha_{m,K_{PL}+1,l}(n)\\ \alpha_{m,K_{PL},l}(n)\end{pmatrix}, \tag{21}$$

$$\overline{\mathbf{A}}_l(m,n)=\begin{pmatrix}\overline{\alpha}_{m,-K_{PL}+1,l}(n)\\ \overline{\alpha}_{m,-K_{PL}+2,l}(n)\\ \vdots\\ \overline{\alpha}_{m,0,l}(n)\\ \vdots\\ \overline{\alpha}_{m,K_{PL}+1,l}(n)\\ \overline{\alpha}_{m,K_{PL},l}(n)\end{pmatrix}, \tag{22}$$

where

$$\overline{\alpha}_{m,v,l}(n)=\overline{\alpha}_{m,1-v,l}(n)$$
$$=\frac{\overline{\alpha}_{m,v,l}(n)+\overline{\alpha}_{m,1-v,l}(n)}{2} \tag{23}$$

$\boldsymbol{A}_l(m, n)$ is updated at the 2ndstage adaptive filter as the same algorithm, described by Eq.(15) as for the time-multiplexed pilot channel structure.

5. Computer Simulations

The BER performances on the reverse link achievable with proposed scheme using the time-multiplex and parallel pilot channel structure were evaluated by computer simulations. Table 1 lists the simulation parameters. SIR based fast TPC [15], [16] is employed with 1 slot delay and 1dB step size. In this paper, a single user is considered. Moreover, the results obtained here can be applied multi-user case since interference from other users can be assumed to collectively become Gaussian noise. Convolutional coding has code generator polynomial of 171, 133 and 165 in the octal notation with coding rate of 1/3 and constraint length of 7 bits. Chip, symbol, and frame timing synchronization are assumed to be perfect at the receiver.

Table 1 Simulation parameters.

Processing gain	96 (64 x 3 / 2)
Spreading code	Orthogonal Gold-sequences
Modulation	QPSK(data) QPSK(spreading)
Fast TPC	SIR-based closed loop
Pilot channel	10% power allocation (time-multiplexed : N_p=4, N_d=36)
Channel coding	Convolutional coding /soft-decision Viterbi decoding (R=1/3,K=7)
Diversity	2 branch 4finger Rake
Interleave size	16 x 72 bits(time multiplexed) 16 x 80 bits(parallel pilot)
Channel Model	2-path Rayleigh fading Vehicular B Rayleigh fading

5.1 Convergence of Channel Estimation Filter Coefficients

Figures 4 show the convergence properties of $\alpha_{N_d/2,0,l}(n)$ ($\alpha_{N_d/2,1,l}(n)$) and $\alpha_{N_d/2,-K_{TM}+1,l}(n)$ ($\alpha_{N_d/2,K_{TM},l}(n)$) for the time-multiplexed pilot channel structure (K_{TM}=3) with m as a parameter. 2-path Rayleigh fading channel was assumed. Initial filter coefficients are $\mathbf{A}_l^T(n)$={0.08 0.17 0.25 0.25 0.17 0.08} which have been optimized to minimize the average BER with a cut and try approach by a computer simulation for the case of normalized maximum Doppler frequency $f_D T_{slot}$ = 0.1. In slow fading (see Fig. 4(a)), the filter coefficients converge to almost the same value when m=10^{-3} is used. In the case of fast fading, on the other hand, $\alpha_{N_d/2,0,l}(n)$ converges to 0.32 and $\alpha_{N_d/2,-K_{TM}+1,l}(n)$ to around 0. These are the desired results (the value of $\alpha_{N_d/2,-K_{TM}+1,l}(n)$ must be much smaller than that of $\alpha_{N_d/2,0,l}(n)$ for faster fading). It is observed that the use of m=0.01 yields unstable filter coefficients and that the use of m=0.0001 gives very slow convergence property. Therefore, the following simulation used m =0.001.

5.2 Observation Interval

5.2.1 Time-Multiplexed Pilot Channel

Increasing the value of K_{TM} improves the SNR of the channel estimate. However, in very fast fading environments, the filter coefficients $\alpha_{m',-K_{TM}+1,l}(n)$ (and $\alpha_{m',K_{TM},l}(n)$) may become unstable. Therefore, the impact of K_{TM} on the achievable BER performance is investigated. Figure 5 plots the average BER performance with K_{TM} as the parameter for 2-path Rayleigh fading channel with $f_D T_{slot}$ = 0.003125 and 0.2. Figure 6 plots the impact of K_{TM} on the average E_b/N_0 per antenna required for achieving average BER=10^{-3}, where K_{TM}=1 means the non-adaptive simple averaging of pilot symbols of two consecutive slots. Also plotted in Fig. 6 are the performances of ideal channel estimation and previously proposed non-adaptive WMSA(K_{TM}=2) channel estimation filter [14] as a reference for comparison. From Figs. 5 and 6, the BER performances are improved as K_{TM} increases in slow fading because the SNR of channel estimate is improved. For example, the performances of K_{TM}=4 and 5 are improved by 1 dB compared to that of K_{TM}=1 and by 0.4 dB compared to that of K_{TM}=2. The performances of K_{TM}=4 and 5 are degraded only by 0.2 dB from the ideal estimation for the range of $f_D T_{slot}$ values less than 0.05. Moreover, in the fast fading, the performances are almost the same regardless of K_{TM}. Since

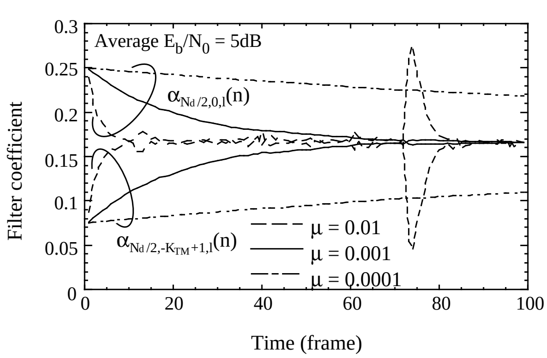

(a) $f_D T_{slot}$ = 0.003125

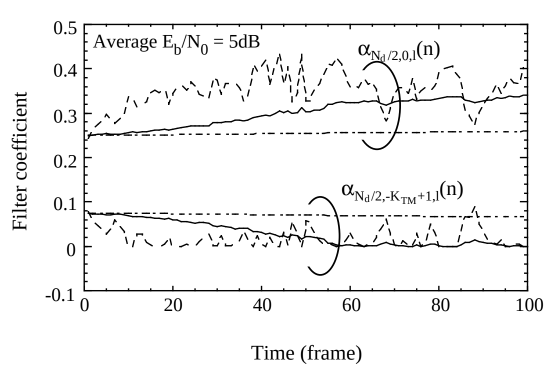

(b) $f_D T_{slot}$= 0.2

Fig. 4 Convergence property.

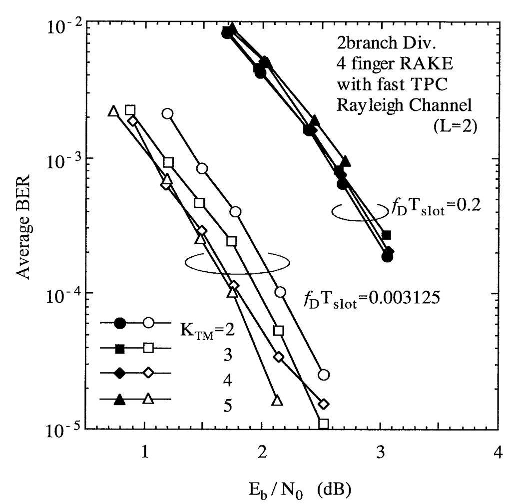

Fig. 5 Impact of K_{TM} on average BER performance. Time-multiplexed pilot.

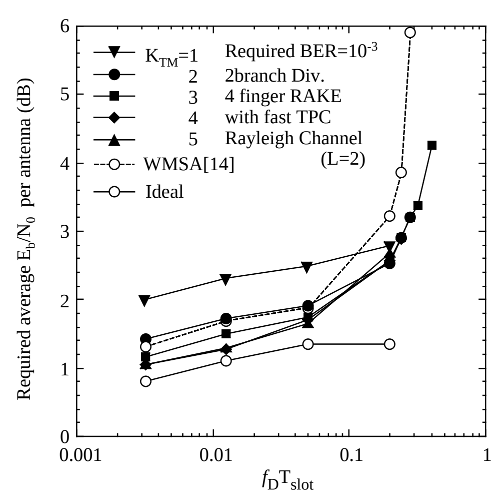

Fig. 6 Impact of K_{TM} on average required E_b/N_0. Time-multiplexed pilot.

the filter coefficients are not stable with $K_{TM} \geq 4$ when the $f_D T_{slot} > 0.3$, K_{TM}=3 can be considered the best.

5.2.2 Parallel Pilot Structure

In parallel pilot channel structure, we first accumulate U pilot symbols. As the value of U decreases, the tracking against fading becomes faster, however the SNR of each instantaneous channel estimate becomes lower. Therefore, U is an important design parameter. Figure 7 plots the impact of U on the average required E_b/N_0 per antenna for achieving average BER=10^{-3}, where $2K_{PL} \cdot U$ is kept constant as 240. For the comparison, performances of ideal channel estimation and non adaptive channel estimation filter [16] are also plotted. The results show that the performances are almost the same in slow fading. As $f_D T_{slot}$ increases, however smaller U provides a better performance.

Next, the impact of K_{PL} is investigated. Figure 8 plots the average BER performances with K_{PL} as a parameter for 2-path Rayleigh fading channel with $f_D T_{slot}$ = 0.003125 and 0.2. U = 20 is used. Figure 9 plots the impact of K_{PL} on the average required E_b/N_0 per antenna for achieving average BER=10^{-3}. Also plotted are the performances of ideal channel estimation and previously proposed non adaptive channel estimation filter [16]. Since the performance with K_{PL} =4 is inferior to other K_{PL} cases in slow fading, K_{PL} =6 can be considered to be optimum and was used in following simulation.

5.3 Performance Comparison

So far, we assumed a 2-path Rayleigh fading channel only. We also evaluated the performance assuming the Vehicular-B Rayleigh fading channel model [17]. Figure 10 compares the average BER performances achievable with adaptive and non-adaptive channel estimation filter for the cases of $f_D T_{slot}$ = 0.003125 and 0.28. Figure 11 compares the average E_b/N_0 per antenna required for achieving average BER=10^{-3}. It is seen from Figs. 6, 9 and 11 that, in the case of slow fading ($f_D T_{slot}$ = 0.003125), compared the non-adaptive channel estimation filter the proposed adaptive channel estimation filters can reduce the required E_b/N_0 by about 0.2 dB for both pilot

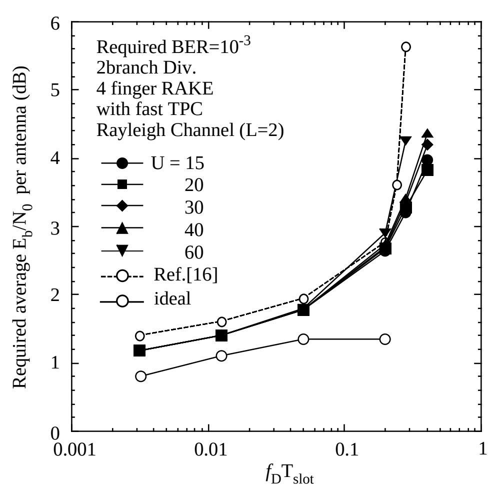

Fig. 7 Impact of U on average required E_b/N_0. Parallel pilot.

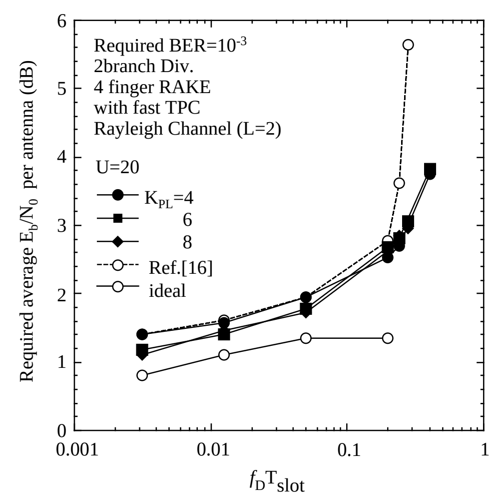

Fig. 9 Impact of K_{PL} on average required E_b/N_0. Parallel pilot.

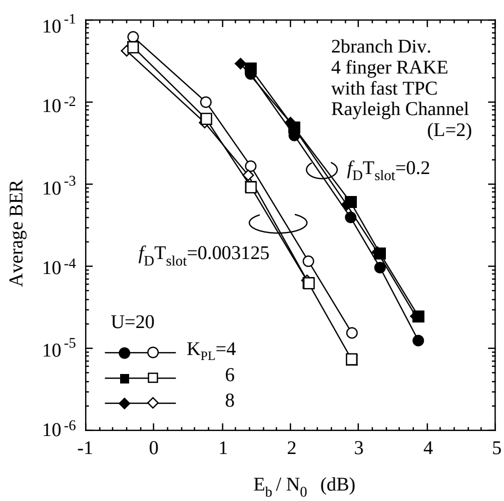

Fig. 8 Impact of K_{PL} on average BER performance. Parallel pilot.

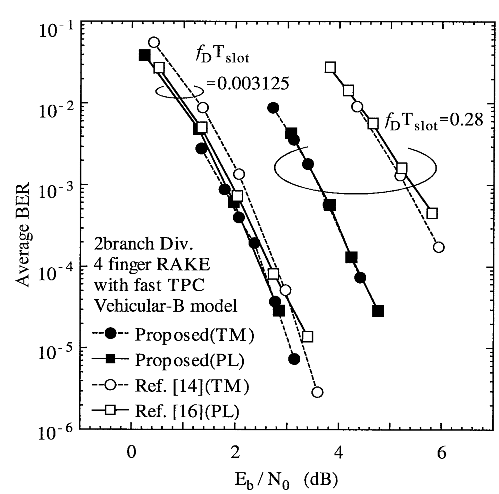

Fig. 10 BER in Vehicular B Rayleigh fading channel.

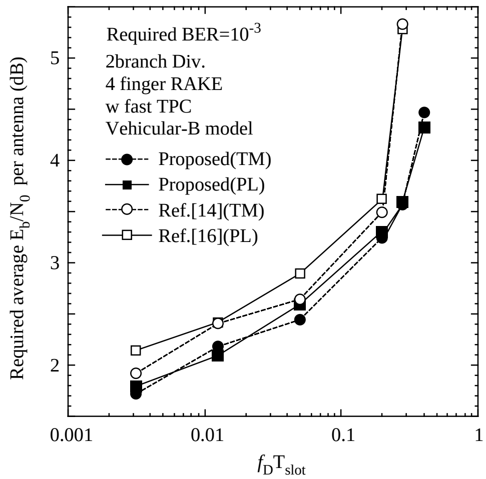

Fig. 11 Required E_b/N_0 in Vehicular B Rayleigh fading channel.

structures under 2-path Rayleigh fading and by 0.4 dB under Vehicular B Rayleigh fading. The E_b/N_0 reduction can be significant in the case of fast fading environments. The required E_b/N_0 reduction can be as much as 2 dB when $f_D T_{slot} = 0.28$. It becomes more than 7 dB when $f_D T_{slot} = 0.4$ (we also computer simulated to find that required E_b/N_0 for achieving average BER=10^{-3} is about 12 dB when non-adaptive channel estimation filters are used). It should be pointed out that the performances achievable with the proposed adaptive filters are almost same from slow to fast fading rate for wide range of f_D values.

6. Conclusion

Adaptive channel estimation filters are presented for coherent DS-CDMA reverse link using time-multiplexed pilot and parallel pilot structures. A pragmatic approach was used in this paper to derive adaptive channel estimation filter. The filter coefficients are updated based on the measured autocorrelation function of the instantaneous channel estimate. The achievable BER performances with fast TPC under multipath Rayleigh fading environments were evaluated by computer simulations. The proposed adaptive channel estimation filter can achieve 0.4 dB superior BER performance in slow fading environment and more than 2.0 dB superior performance in fast fading environment to previously proposed non-adaptive channel estimation filters. Moreover, the average BER performances achievable with proposed adaptive channel estimation filters scheme for both time-multiplexed and parallel pilot structures are almost same for wide range of f_D values.

References

[1] F.Adachi, M.Sawahashi, and H.Suda, “Wideband DS-CDMA for next-generation mobile communications systems,” IEEE Commun., Mag., vol. 36, pp.56-69, Sept. 1998.
[2] F.Adachi and M.Sawahashi, “Wideband wireless access based on DS-CDMA,” IEICE Trans. Commun., vol.E81-B, no.7, pp.1305-1316, July 1998.
[3] A.J.Viterbi, CDMA: Principles of spread spectrum communications, Addison Wesley, 1995.
[4] R.Kohno, R.Meiden, and L.B.Milstein, “Spread spectrum access methods for wireless communications, ” IEEE Commun. Mag., vol.33, no.1, pp.58-67, Jan. 1995.
[5] A.Baier, U.C.Fiebig, W.Granzaow, W.Koph, P.Teder, and J.Thielecke, “Design study for a CDMA-based third-generation mobile radio system,” IEEE J. Sel. Areas Commun., vol.SAC-12, no.5, pp.733-743, May 1994.
[6] T.Westman and H.Holma, “CDMA system for UMTS high bit rate service,” Proc. 47th IEEE Veh. Technol. Conf., pp.825-829, Phoenix, U.S.A., May 1997.
[7] M.Ewerbring, J.Farjg, and W.Granzow, “Performance evaluation of a wideband tsetbed based on CDMA,” ibid., pp.1009-1013.
[8] K.Miya, M.Watanabe, M.Hayashi, T.Kitade, O.Kato, and K.Homma, “CDMA/TDD cellular systems for the 3rd generation mobile communications,” ibid., pp.820-824.
[9] W.C.Jakes Jr., ed., Microwave mobile communicants, Wiley, New York, 1974.
[10] S.Sampei and T.Sunaga, “Rayleigh fading compensation for QAM in land mobile radio communications,” IEEE Trans. Veh. Technol., vol.VT-42, pp.137-147, May 1993.
[11] F.Ling, “Coherent detection with reference-symbol based estimation for direct sequence CDMA uplink communications,” Proc. VTC’93, pp.400-403, New Jersey, USA, May 1993.
[12] S.Abeta, S.Sampei, and N.Morinaga, “ DS/CDMA coherent detection system with a suppressed pilot channel,” Proc. IEEE GLOBECOM’94, pp.1622-1626, Dec. 1994.
[13] A.Higashi, T.Taguchi, and K.Ohno, “ Performance of coherent detection and RAKE for DS-CDMA up-link channels,” Proc. IEEE PIMRC’95, pp.436-440, Toronto, Canada, Sept. 27-29, 1995.
[14] H.Andoh, M.Sawahashi, and F.Adachi, “ Channel estimation filter using time-multiplexed pilot channel for coherent rake combining in DS-CDMA mobile radio,” IEICE Trans. Commun., vol.E81-B, no.7, pp.1517-1526, July 1998.
[15] S.Seo, Y.Okumura, T.Dohi, and F.Adachi, “SIR-based transmit power control of reverse link for coherent DS-CDMA mobile radio,” IEICE Trans. Commun., vol.E81-B, no.7, pp.1508-1516, July 1998.
[16] S.Abeta, M.Sawahashi, and F.Adachi, “Performance comparison between time-multiplexed pilot channel and parallel pilot channel for coherent rake combining is DS-CDMA mobile radio,” IEICE Trans. Commun., vol.E81-B, no.7, pp.1417-1425, July 1998.
[17] Procedure for evaluation of transmission technologies for FPLMTS, ITU-R TG8-1/TEMP/223-E. Sept. 1995.

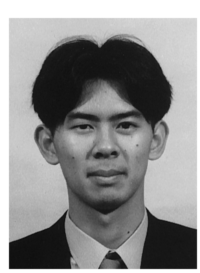

Sadayuki Abeta received the B.E., M.E. and Ph.D. degrees in electical communication engineering from Osaka University, Osaka, Japan, in 1993, 1995, and 1997 respectively. In 1997, he joined NTT Mobile Communications Network, Inc. His reseach interests include digital mobile communication systems and spread spectrum. Dr. Abeta is a member of IEEE.

Mamoru Sawahashi received the B.S. and M.S. degrees from the University of Tokyo, Tokyo, Japan. In 1985, he joined NTT Laboratories, and in 1992, he transferred to NTT Mobile Communications Network, Inc. Since joining NTT, he has been engaged in the research and development of modem technique for mobile radio communications, and code synchronization and interference canceller technique for DS-CDMA. He is now a Senior Research Engineer with the Research and Development Department of NTT Mobile Communications Network, Inc.

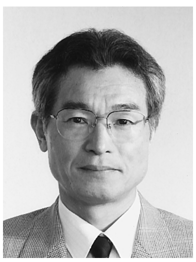

Fumiyuki Adachi graduated from Tohoku University, Japan in 1973 and received the Dr. Eng. degree from the same University in 1984. In 1973, he joined Nippon Telegraph & Telephone Corporation (NTT) Laboratories in Japan and in 1992, he transferred to NTT Mobile Communications Network, Inc. At NTT, he worked for the development of a TDMA digital cellular base station transceiver. At present, he is a senior executive research engineer at NTT Mobile Communications Network, Inc. and has been leading a research group for wideband DS-CDMA mobile radio. His research interests also include bandwidth efficient modulation/demodulation, diversity reception, and channel coding. During the academic year of 1984/85, he was a United Kingdom SERC Visiting Research Fellow in the Department of Electrical Engineering and Electronics of Liverpool University. Since 1997, he is a visiting professor at Nara Institute of Science and Technology. He has written chapters of three books: Y. Okumura and M. Shinji, eds., “Fundamentals of mobile communications” published in Japanese by IEICE, 1986; M. Shinji, ed., “Mobile communications” published in Japanese by Maruzen Publishing Co., 1989; and M. Kuwabara, ed., “Digital mobile communications” published in Japanese by Kagaku Shinbun-sha, 1992. He was co-recipient of the IEICE Paper of the Year Award in 1997. He was co-recipient of the IEEE Vehicular Technology Society Paper of the Year Award in 1980 and 1990 and was a secretary of IEEE Vehicular Technology Society Tokyo Chapter from 1991 to 1994.